Applied Catalysis A: General 413–414 (2012) 176–182

Contents lists available at SciVerse ScienceDirect

Applied Catalysis A: General

journal homepage: www.elsevier.com/locate/apcata

Study of the interaction between hydrogen and the MoO_3–ZrO_2 catalyst

Nurun Najwa Ruslan [a], Sugeng Triwahyono [a,*], Aishah Abdul Jalil [b], Sharifah Najiha Timmiati [b], Nur Hazirah Rozali Annuar [a]

[a] Ibnu Sina Institute for Fundamental Science Studies, Faculty of Science, Universiti Teknologi Malaysia, 81310 UTM Skudai, Johor, Malaysia
[b] Department of Chemical Engineering, Faculty of Chemical Engineering, Universiti Teknologi Malaysia, 81310 UTM Skudai, Johor, Malaysia

ARTICLE INFO

Article history:
Received 6 September 2011
Received in revised form 21 October 2011
Accepted 5 November 2011
Available online 15 November 2011

Keywords:
MoO_3–ZrO_2
Proton
Electron
Surface diffusion
n-Heptane isomerization

ABSTRACT

The interaction of molecular hydrogen with the surface of MoO_3–ZrO_2 was observed using infrared IR and electron spin resonance (ESR) spectroscopy, and the hydrogen adsorption was quantitatively evaluated in the temperature range of 323–573 K. The hydrogen adsorbed IR results confirmed the formation of a new broad band in the range of 3700–3400 cm^{-1}, which corresponds to hydrogen-bonded OH groups. A decrease in the ESR signals indicated the formation of electrons that have been trapped by the electron-deficient metal cations and/or oxygen radicals. The hydrogen adsorbed IR and ESR results suggested that the protons and electrons were formed on the surface of MoO_3–ZrO_2 from molecular hydrogen enhancing the isomerization of *n*-heptane. A quantitative study of the hydrogen adsorption showed that the rate of hydrogen uptake was high for the first few minutes at 473 K and above, and the rate reached an equilibrium value within 10 h. At 423 K, different features of the hydrogen adsorption were observed on MoO_3–ZrO_2, where the hydrogen uptake increased slowly with time and did not reach equilibrium after 10 h. The rate of hydrogen adsorption increased slightly at 373 K and below. Hydrogen adsorption on MoO_3–ZrO_2 involves two successive steps. The first step involves hydrogen dissociation on a specific site on the MoO_3–ZrO_2 catalyst to form hydrogen atoms, and the second step involves the surface diffusion of the hydrogen atoms on the MoO_3–ZrO_2 surface. Then the hydrogen atom becomes a proton by donating an electron to an adjacent Lewis acid site. The rate-controlling step involves the surface diffusion of hydrogen atoms and has an activation energy of 62.8 kJ/mol. A comparison of the hydrogen adsorption on SO_4^{2-}–ZrO_2, WO_3–ZrO_2 and MoO_3–ZrO_2 catalysts is discussed.

1. Introduction

Solid acid catalysts based on zirconia, such as SO_4^{2-}–ZrO_2, WO_3–ZrO_2 and MoO_3–ZrO_2 catalysts, have been extensively investigated due to their outstanding catalytic properties (e.g., activity, stability and regeneration as solid acid catalysts) [1–3]. These catalysts possess strong acid sites and exhibit high activity for acid-catalyzed reactions in the presence of hydrogen. The major differences between the SO_4^{2-}–ZrO_2, WO_3–ZrO_2 and MoO_3–ZrO_2 catalysts are that WO_3–ZrO_2 and MoO_3–ZrO_2 do not suffer from metal oxide losses during treatment and exhibit high thermal stability compared to SO_4^{2-}–ZrO_2 [2,4–6]. Several research groups have reported the preparation method, activation mode, the role of active sites (e.g., Pt), the role of hydrogen gas and catalytic tests for acid-catalyzed reactions. Our research group has reported the role of hydrogen in the dynamic modification of active sites by molecular hydrogen [7–9] and the quantitative analysis of hydrogen adsorption [10,11] for the SO_4^{2-}–ZrO_2, WO_3–ZrO_2 and MoO_3–ZrO_2 catalysts. The catalysts follow the concept of "*Molecular hydrogen-originated protonic acid sites*" in which molecular hydrogen is dissociatively adsorbed on specific active sites, such as Pt or other acidic sites, to form hydrogen atoms that spill over onto the supports and undergo surface diffusion to form protonic acid sites near Lewis acid sites. The hydrogen adsorption continued for a long time, and the hydrogen uptake exceeded the H/Pt ratio of unity for both Pt/SO_4^{2-}–ZrO_2 and Pt/WO_3–ZrO_2. The differences between SO_4^{2-}–ZrO_2 and WO_3–ZrO_2 include the formation temperature of protonic acid sites, the rate-controlling step and the apparent activation energy for hydrogen adsorption. In addition, the Pt sites were found to be indispensable on SO_4^{2-}–ZrO_2, but not on WO_3–ZrO_2.

Recently, the MoO_3–ZrO_2 catalysts have received considerable interest due to their acidic property, high activity and stability, which are similar to the SO_4^{2-}–ZrO_2 and WO_3–ZrO_2 catalysts. Several research groups have reported preparation techniques [12,13], the effect of the Mo loading [14] and catalytic testing for the isomerization of alkanes [15,16] for the MoO_3–ZrO_2 catalysts. Recent studies have shown that the monolayer coverage of molybdate species on the surface of zirconia is responsible for the outstanding properties of the MoO_3–ZrO_2 catalyst. The isomerization of

* Corresponding author. Tel.: +60 7 5536076; fax: +60 7 5536080.
E-mail address: sugeng@utm.my (S. Triwahyono).

0926-860X/$ – see front matter © 2011 Elsevier B.V. All rights reserved.
doi:10.1016/j.apcata.2011.11.007

n-heptane on MoO_3–ZrO_2 has been reported by Yori et al. [15], who showed that the activity and stability of the catalyst depends on the MoO_3 content, the structure of the molybdate species on the surface of zirconia and the presence of a H_2 or N_2 carrier gas. The presence of hydrogen increases the conversion of *n*-heptane and the selectivity for the C_8 isomer, whereas while the high C_7 isomer selectivity is achieved in the presence of nitrogen on MoO_3–ZrO_2 samples calcined at 973 K. The isomerization of *n*-hexane on MoO_3–ZrO_2 samples at low temperatures has been reported by Arata [16]. Kenney et al. [17] reported the promotive effect of hydrogen on the conversion of methylcyclopentane over MoO_3–ZrO_2 in which hydrogen was involved in the ring-opening and cracking reactions. Our research group has also reported the activity of MoO_3–ZrO_2 for the isomerization of *n*-heptane. The presence of a tetragonal ZrO_2 phase corresponding to strong Lewis acid sites is responsible for the high activity and stability of MoO_3–ZrO_2 due to its ability to facilitate the formation of protonic acid sites via the hydrogen spillover mechanism [9].

Although extensive research has been focused on the preparation, characterization and catalytic activity of MoO_3–ZrO_2 catalysts, there are no reports on the interaction of hydrogen atoms with the surface of MoO_3–ZrO_2. In the present work, we report the interaction of molecular hydrogen and the surface of MoO_3–ZrO_2 with ESR and IR spectroscopy, and we quantitatively evaluated the hydrogen adsorption to determine the rate of hydrogen adsorption, the rate-controlling step and the apparent activation energy involved in the adsorption process. A comparison of the hydrogen adsorption on MoO_3–ZrO_2, SO_4^{2-}–ZrO_2 and WO_3–ZrO_2 is discussed.

2. Experimental

2.1. Catalyst preparation

Zirconium hydroxide ($Zr(OH)_4$) was prepared from an aqueous solution of $ZrOCl_2 \cdot 8H_2O$ by hydrolysis with an aqueous solution of NH_4OH at pH 9.0 [18]. The precipitate was filtered and washed with double distilled water followed by drying at 383 K to form zirconium hydroxide. ZrO_2 was prepared by calcination of $Zr(OH)_4$ at 873 K for 3 h. MoO_3 was prepared by calcination of H_2MoO_4 at 673 K for 3 h. The MoO_3–ZrO_2 sample was prepared by impregnation of $Zr(OH)_4$ with an aqueous solution of ammonium heptamolybdate ($[NH_4]_6Mo_7O_{24}$) followed by drying at 383 K and calcination in air at 1093 K. The surface area of the MoO_3–ZrO_2 was 56 m^2/g, and the content of Mo was 5 wt%.

2.2. IR measurements

For measurement of the IR spectra, a self-supported wafer was placed in an in situ stainless steel IR cell with CaF_2 windows and outgassed at 623 K for 3 h [19]. In the H_2-exposure experiments, the sample was exposed to 6.7 kPa of hydrogen at room temperature. The sample was heated stepwise from room temperature to 423 K in 50 K increments. All of the spectra were recorded on a Perkin-Elmer Spectrum GX FT-IR Spectrometer at room temperature.

2.3. Electron spin resonance

A JEOL JES-FA100 ESR spectrometer was used to observe the formation of unpaired electrons during the in vacuo heating and to observe the interaction of the unpaired electrons with electrons formed from molecular hydrogen at room temperature to 473 K. The catalyst was outgassed at 623 K for 3 h followed by the introduction of 6.7 kPa of gaseous hydrogen at room temperature. Then the catalyst was heated to room temperature, 323, 373, 423 and 473 K in the presence of hydrogen. All signals were recorded at room temperature.

2.4. Hydrogen adsorption

The hydrogen adsorption was carried out with the automatic gas adsorption apparatus Bellsorp 28SA. A sample (300 mg) was placed in an adsorption vessel and pretreated at 623 K for 6 h under hydrogen stream followed by outgassing at 623 K for 6 h. Next, it was cooled to an adsorption temperature and held at this temperature for 3 h [20,21]. The adsorption temperature varied from 323 to 573 K. Then hydrogen was introduced into the adsorption system at 6.7 kPa, and the pressure change was monitored as a function of time to calculate the hydrogen uptake.

2.5. Isomerization of n-heptane

The isomerization of *n*-heptane was performed in a continuous flow reactor at 573 K [22]. Prior to the isomerization, the catalyst was activated in an oxygen stream at 623 K for 1 h. The catalyst was subsequently heated in a hydrogen stream at 623 K for 3 h and then cooled to 573 K in a hydrogen stream. A dose of *n*-heptane (43 μmol) was passed over the 0.4 g of activated catalyst, and the products were trapped at 77 K before being flash-evaporated into an online 6090N Agilent gas chromatograph equipped with a VZ-7 packed column and an FID detector.

The yield of the reaction was determined by the products formed from the conversion of *n*-heptane and the selectivity to *iso*-heptane. The conversion and selectivity were calculated according to Eqs. (1) and (2), respectively,

$$X = \frac{\sum A_i - A_{n\text{-heptane}}}{\sum A_i} \times 100\%; \quad (1)$$

$$S_{iso} = \frac{\sum A_i}{\sum A_i - A_{n\text{-heptane}}} \times 100\%, \quad (2)$$

where A_i is the corrected chromatographic area for a particular compound.

3. Results

Fig. 1 shows the background-corrected IR spectra of MoO_3–ZrO_2 in the OH stretching region for the catalyst outgassed at 623 K for 3 h followed by heating in the presence of hydrogen at different temperatures. The interaction of gaseous hydrogen with the surface of the MoO_3–ZrO_2 produced a new broad band in the region of 3700–3400 cm^{-1}, which corresponds to hydrogen-bonded OH groups. This broad band intensified at elevated temperatures, indicating that the OH groups were formed by heating in the presence of hydrogen gas.

Fig. 2A shows the ESR signals of the outgassed MoO_3–ZrO_2 maintained at (a) room temperature and (b) 623 K for 3 h followed by heating in the presence of hydrogen at different temperatures (spectra c to g). Fig. 2B shows a magnification of the ESR signal (a) in Fig. 2A. The signal consists of the low intensity peaks related to hexa- ($g_\perp = 1.93$), penta- ($g_\perp = 1.95$) and tetra- ($g_\perp = 1.91$) coordinated Mo^{5+} species [23–25] as well as Zr^{3+} ion [23,26]. As the MoO_3–ZrO_2 was outgassed at 623 K for 3 h, the peaks for the Mo^{5+} species and the Zr^{3+} ion intensified. In addition, a new peak corresponding to an oxygen radical appeared at $g_\perp = 1.99$ and 2.01 [26,27], which is due to heating in vacuo and dehydroxylation of the MoO_3–ZrO_2, leaving unpaired electrons localized on the electron-deficient metal cations and/or oxygen radicals. The introduction of gaseous hydrogen followed by heating resulted in the formation of electrons and protons where the electrons were trapped by the electron-deficient metal cations and/or oxygen radicals, resulting

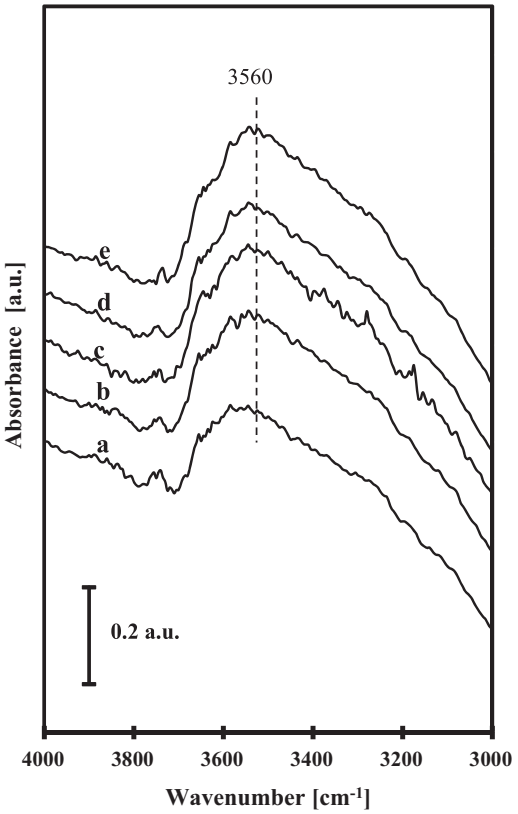

Fig. 1. Changes in the IR spectra when the sample was (a) activated at 598 K and exposed to hydrogen at (b) room temperature, (c) 323 K, (d) 373 K, and (e) 423 K.

in reduction of the ESR signals from Mo^{5+} species, Zr^{3+} ions and oxygen radicals. In addition, the protons were stabilized near the surface oxygen atoms as hydrogen-bonded OH groups. At 473 K, the intensity of the ESR signals was nearly restored to the initial ESR signals of the MoO_3–ZrO_2, indicating a reduction in the number of unpaired electrons in the catalyst.

Fig. 3 shows the variation in hydrogen uptake on ZrO_2 and MoO_3–ZrO_2 as a function of time at 423 K. For the MoO_3–ZrO_2, hydrogen uptake continued for more than 10 h. Hydrogen uptake reached 1.21×10^{19} H-atom/g-cat for MoO_3–ZrO_2 in 10 h. In contrast, only a trace amount of hydrogen uptake was observed for the ZrO_2 samples. These results clearly indicated that the presence of MoO_3 is indispensable for increasing the hydrogen uptake rate on a ZrO_2 support. The variations in the hydrogen uptake on MoO_3–ZrO_2 as a function of time at different temperatures are shown in Fig. 4. At 473 and 573 K, fast adsorption occurred in the first few minutes followed by slower adsorption until equilibrium was reached within 10 h. At 423 K, hydrogen adsorption continued but did not reach equilibrium even after 10 h. At temperatures of 373 K and below, hydrogen uptake increased with temperature to a lesser extent. We suggest that temperatures above 423 K are required for hydrogen adsorption on MoO_3–ZrO_2 to cross over the energy barrier at an appreciable rate.

The effect of gaseous hydrogen on the catalytic activity of the MoO_3–ZrO_2 is shown in Fig. 5. The presence of hydrogen gas enhanced and stabilized the catalytic activity of the MoO_3–ZrO_2, where the conversion of *n*-heptane and the selectivity for *iso*-heptane at 573 K were approximately 32% and 44.5%, respectively. We suggest that the presence of hydrogen in the gas phase provided active protonic acid sites, which are required for the initiation of the isomerization, via the hydrogen spillover mechanism. In fact, no isomer product was observed when the hydrogen carrier gas was switched to nitrogen. The activity of MoO_3–ZrO_2 recovered to almost 85% of the original activity after the carrier gas was switched back to hydrogen.

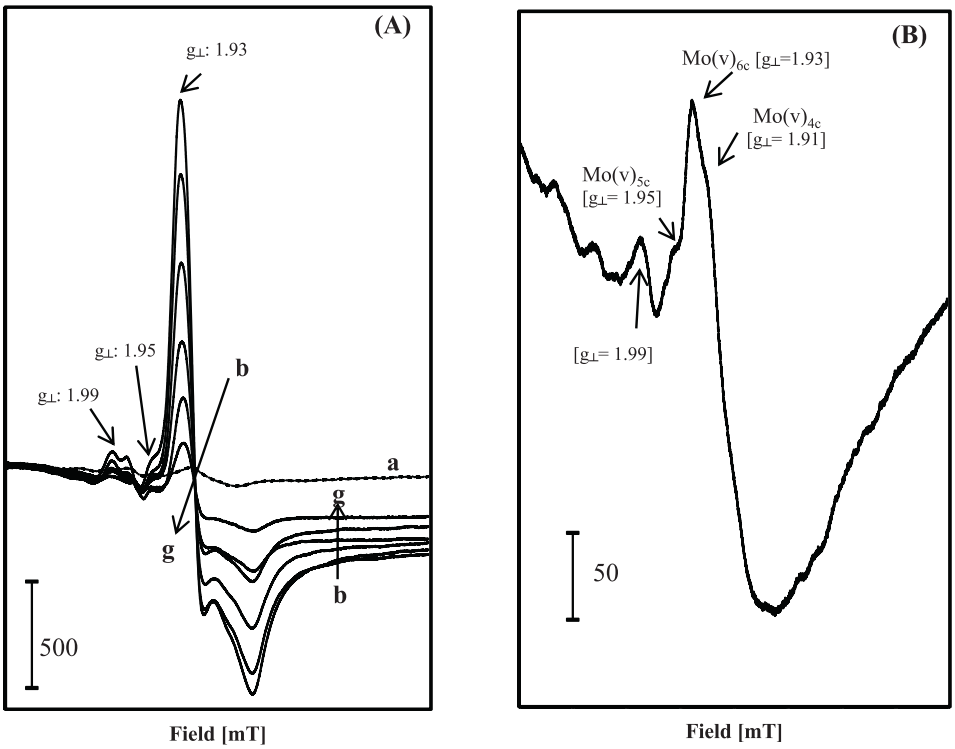

Fig. 2. (A) ESR spectra of MoO_3–ZrO_2 outgassed at (b) 673 K for 3 h. 100 Torr of hydrogen was adsorbed at (c) room temperature, (d) 323 K, (e) 373 K, (f) 423 K, and (g) 473 K. (a) Spectrum of MoO_3–ZrO_2 before outgassing. (B) Enlargement of spectrum (a) in (A).

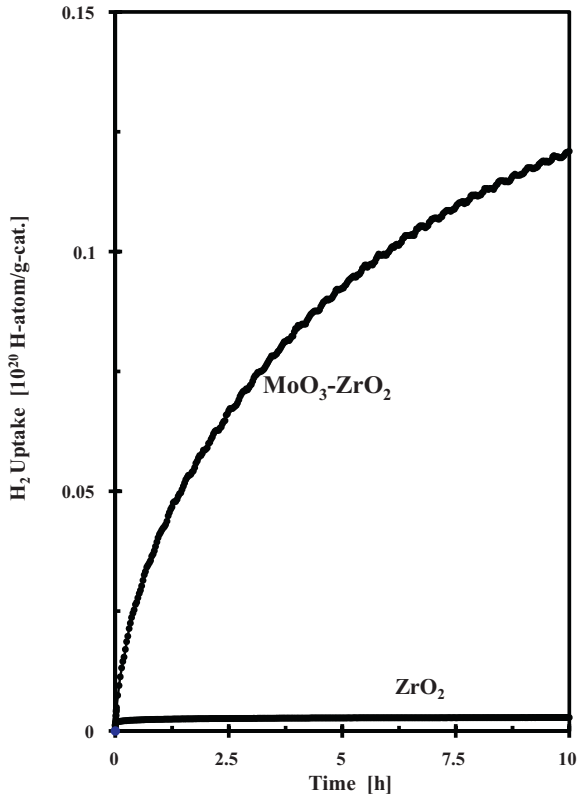

Fig. 3. Variation in the hydrogen uptake as a function of time at 423 K for ZrO_2 and MoO_3–ZrO_2.

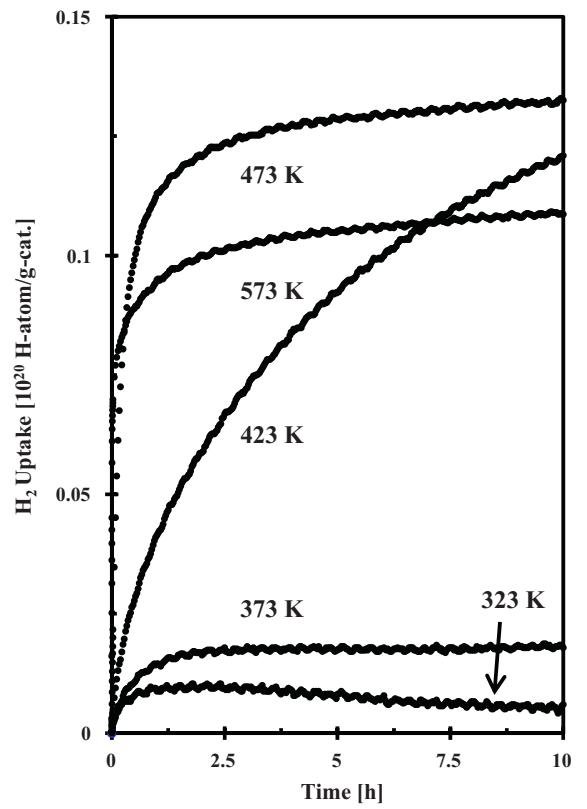

Fig. 4. Variation in the hydrogen uptake on MoO_3–ZrO_2 as a function of time at different temperatures.

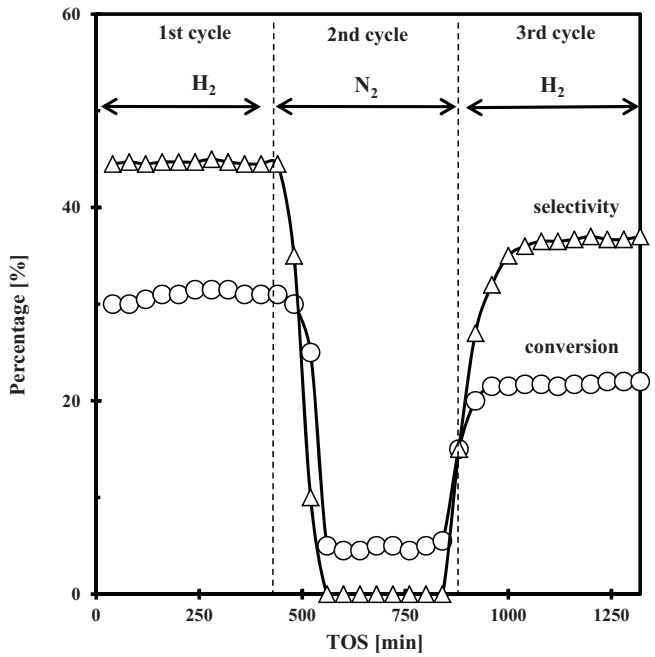

Fig. 5. Effect of the presence of hydrogen in the isomerization of *n*-heptane over MoO_3–ZrO_2 at 573 K.

4. Discussion

The characteristic features of hydrogen interaction with MoO_3–ZrO_2 are summarized as follows:

1. IR spectra showed that heating in the presence of molecular hydrogen resulted in a broad band centered at 3560 cm^{-1}, which has been assigned to hydrogen-bonded OH groups.
2. Heating in the presence of molecular hydrogen decreased the ESR signals, which indicated a perturbation of the electron-deficient metal cations or oxygen radicals by electrons from the hydrogen atoms.
3. The rate of hydrogen uptake on the MoO_3–ZrO_2 was faster than was observed for ZrO_2.
4. On MoO_3–ZrO_2, the hydrogen adsorption reached equilibrium within 10 h at 473 K and above, whereas it continued to increase without reaching an equilibrium after 10 h at 423 K.
5. At 373 K and below, hydrogen uptake was minimal for MoO_3–ZrO_2.

The IR and ESR results showed that protons and electrons from gaseous hydrogen were formed at elevated temperature on MoO_3–ZrO_2. As shown in Fig. 1, a broad band in the range of 3700–3400 cm^{-1}, ascribed to hydrogen-bonded OH groups, was formed by heating the sample in the presence of gaseous hydrogen. Based on the unchanged band at >3700 cm^{-1}, the OH groups formed from the hydrogen in gas phase were not isolated, but the OH groups might interact with some species on the surface of the MoO_3–ZrO_2. These OH groups may be attributed to the Brönsted Mo–OH acid groups on the sample surface [28]. Molecular hydrogen may be dissociatively adsorbed on specific active sites, such as reduced metals or acidic sites, to form hydrogen atoms, which donate electrons to form protons that bond with Mo atoms through oxygen atoms. The resulting electrons are trapped by the electron-deficient metal cations and/or oxygen radicals, causing a reduction in the ESR signals from the Mo^{5+} species, Zr^{3+} ions and oxygen radicals.

Our research group has previously reported kinetic studies of hydrogen adsorption on Pt/SO_4^{2-}–ZrO_2 [10] and Pt/WO_3–ZrO_2 [11]. The hydrogen adsorption on Pt/SO_4^{2-}–ZrO_2 was characterized by dissociative-adsorption of molecular hydrogen on Pt sites and spillover of hydrogen atoms, which was followed by surface diffusion. The hydrogen adsorption on Pt/WO_3–ZrO_2 has been evaluated through two different routes. One route involves adsorption on Pt sites, and the other involves direct adsorption on the WO_3–ZrO_2. The general trends observed for the hydrogen adsorption on the SO_4^{2-}–ZrO_2, WO_3–ZrO_2 and MoO_3–ZrO_2 catalysts were comparable. For certain adsorption temperatures, the hydrogen uptake continued for a long period, and the H/Pt ratio exceeded unity for Pt/SO_4^{2-}–ZrO_2 and Pt/WO_3–ZrO_2. In addition, the similarities between WO_3–ZrO_2 and MoO_3–ZrO_2 were observed for the entire adsorption temperature range. At low adsorption temperatures, low hydrogen uptake was observed, and the rate of hydrogen adsorption increased slightly with increasing temperatures, indicating that there is an activation barrier for adsorption. At relatively high temperatures, the hydrogen adsorption occurred very rapidly and reached equilibrium within a few hours. At equilibrium, the hydrogen uptake was lower at higher temperatures due to the exothermic process of general adsorption.

There are some differences among the SO_4^{2-}–ZrO_2, WO_3–ZrO_2 and MoO_3–ZrO_2 catalysts. Although the hydrogen uptake was negligibly small for SO_4^{2-}–ZrO_2 in the absence of Pt, the hydrogen uptake observed for WO_3–ZrO_2 and MoO_3–ZrO_2 was substantial. WO_3–ZrO_2 and MoO_3–ZrO_2 must possess sites that dissociate hydrogen molecules, whereas SO_4^{2-}–ZrO_2 does not possess these sites. The rate of hydrogen adsorption is also similar for the WO_3–ZrO_2 and MoO_3–ZrO_2 catalysts. On WO_3–ZrO_2 and MoO_3–ZrO_2, fast hydrogen adsorption occurred in the initial period followed by slower hydrogen adsorption until an adsorption equilibrium was established within 10 h at temperatures at 473 K and above. Below 473 K, the hydrogen uptake increased with temperature but did not reach equilibrium after 10 h. The general features of hydrogen adsorption on the WO_3–ZrO_2 and MoO_3–ZrO_2 catalysts were essentially the same for all adsorption temperature ranges. Therefore, it is suggested that the effects of WO_3 and MoO_3 metal oxides on ZrO_2 supports are essentially the same in terms of adsorptivity. Hydrogen adsorption should occur directly on MoO_3–ZrO_2 and WO_3–ZrO_2, although it is not known if the active sites that dissociatively adsorb molecular hydrogen are different from those used in the hydrogen spillover process or if the hydrogen atoms are converted to H^+ or H^- over MoO_3–ZrO_2. Regardless of which active sites dissociatively adsorb molecular hydrogen, we propose that the adsorption of hydrogen on MoO_3–ZrO_2 involves at least two successive steps. First, the molecular hydrogen dissociates to form hydrogen atoms, and then the hydrogen atoms diffuse on the surface. If the active sites responsible for dissociating hydrogen molecules are different from those required for hydrogen atom diffusion, the step involving the transportation of hydrogen atoms from the formation of the hydrogen atoms to the surface diffusion of the hydrogen atoms should be taken into account between the two proposed steps. Even if this transportation step is involved, the steps involving molecular hydrogen dissociation and transformation can be combined and expressed as a single step for hydrogen atom formation.

If hydrogen atom formation is the rate-controlling step, the rate of hydrogen adsorption would be expressed by the first order rate equation [11]

$$\frac{dC}{dt} = k(C_e - C) \tag{3}$$

where C represents the concentration of hydrogen atoms on MoO_3–ZrO_2, which is a constant value for the entire surface of MoO_3–ZrO_2, and C_e represents the concentration of hydrogen atoms on the MoO_3–ZrO_2 catalyst, which has been equilibrated with hydrogen molecules. The concentrations of hydrogen atoms on MoO_3–ZrO_2 at t (C) and equilibrium (C_e) can be represented by the hydrogen uptake on MoO_3–ZrO_2 at t (M) and equilibrium (M_e). Integration of Eq. (3) and the application of the hydrogen uptake values (M and M_e) give

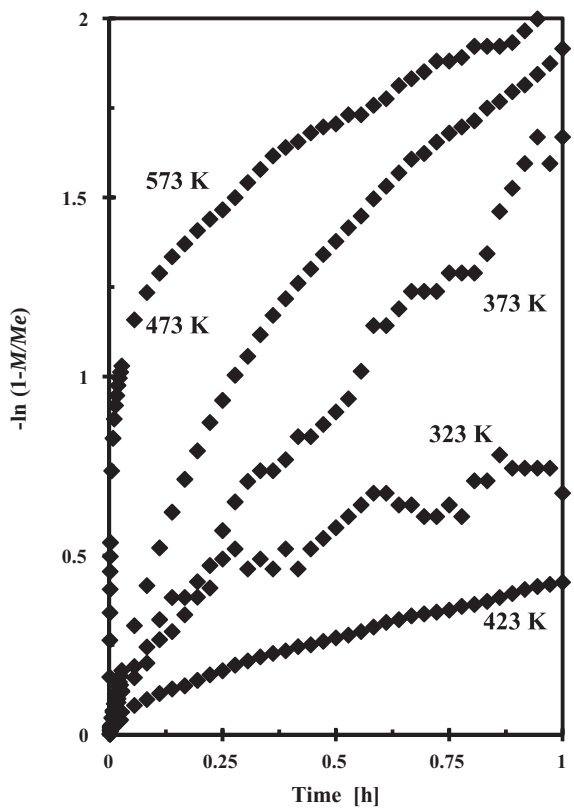

Fig. 6. Plot of $-\ln(1 - M/M_e)$ as a function of t for hydrogen adsorption at different adsorption temperatures for MoO_3–ZrO_2.

$$-\ln\left(1 - \frac{M}{M_e}\right) = kt \tag{4}$$

where M and M_e represent the hydrogen uptake at t and equilibrium, respectively.

The plots of $-\ln(1-M/M_e)$ as a function of t are shown in Fig. 6. We used the value of M at 10 h for M_e at each adsorption temperature because the values of M_e are unknown for adsorption temperatures ≥423 K. Straight lines were obtained only for the adsorptions at 423 K. The plots for the adsorptions at other temperatures deviated greatly from linearity. These results suggest that the step involving hydrogen atom formation is not the rate-controlling step for the adsorption of hydrogen in the temperature range of 323–573 K.

When surface diffusion is the rate-controlling step, the rate of adsorption would be expressed by the equation for Fick's second law of surface diffusion [11]

$$\frac{\partial C}{\partial t} = \frac{D}{r}\left(\frac{\partial}{\partial r}\right)\left(r\frac{\partial C}{\partial r}\right) \tag{5}$$

where C, r and D represent the surface concentration of hydrogen atoms, the distance from the center of the hydrogen dissociation sites and the diffusion coefficient of the hydrogen atom, respectively.

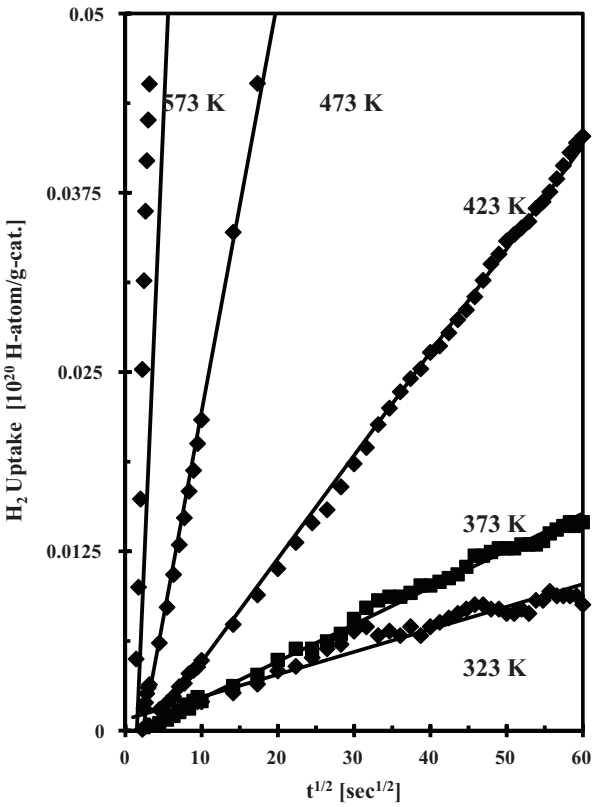

Fig. 7. Plot of the hydrogen uptake on MoO_3–ZrO_2 as a function of the square root of time at different temperatures.

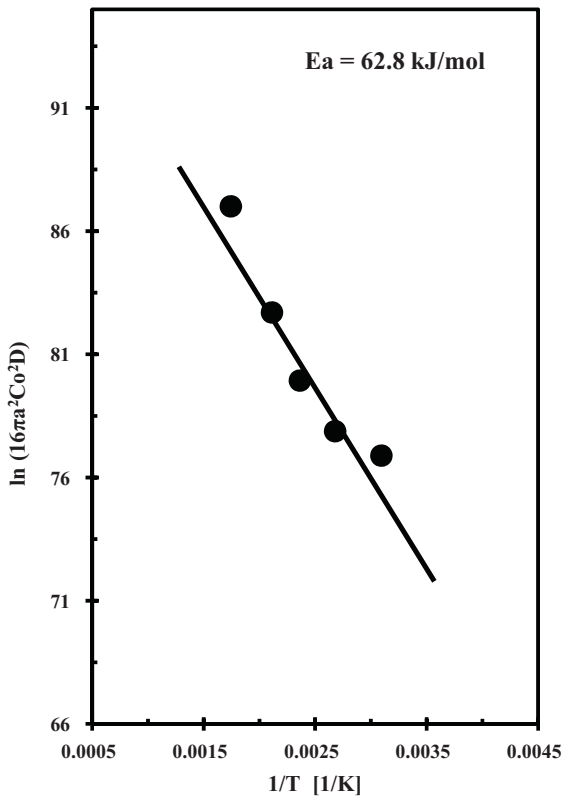

Fig. 8. Plot of $\ln(16\pi a^2 C_0^2 D)$ as a function of $1/T$ for hydrogen adsorption on MoO_3–ZrO_2.

The initial condition is $C=0$ when $t=0$ and $r>a$. The boundary condition is $C=C_0$ when $r=a$ and $t>0$. The introduction of a boundary condition to Eq. (5) yields Eq. (6) when Dt/a^2 is small.

$$C = C_0 a^{1/2} r^{-1/2} erfc\left(\frac{r-1}{4Dt^{-1/2}}\right) \tag{6}$$

The amount of hydrogen atom M can be represented as follows:

$$M = \int_0^t \left[\frac{\partial C}{\partial r|_{r=a}} 2\pi a\right] dt = 4\pi^{1/2} a C_0 D^{1/2} t^{1/2} \tag{7}$$

where M represents the hydrogen uptake (i.e., the amount of diffusing hydrogen atoms).

The plots of M as a function of $t^{1/2}$ for the various adsorption temperatures are shown in Fig. 7; all plots exhibit straight lines. However, the straight lines do not cross the origin due to the unsteady state adsorption of hydrogen during the initial period of adsorption. The slope of the plot of M as a function of $t^{1/2}$ is proportional to the square root of the diffusion constant, D. The activation energy for diffusion is obtained by the Arrhenius plot of the square of the slope. The Arrhenius plot is shown in Fig. 8. The apparent activation energy is 62.8 kJ/mol in the $t^{1/2}$ range of 0–60 $s^{1/2}$.

Our research group has previously reported the adsorption of hydrogen on Pt/SO_4^{2-}–ZrO_2 [10], Pt/WO_3–ZrO_2 [11] and Pt/MoO_3 [21]. The rate-controlling step for the hydrogen adsorption involved the surface diffusion of spilt-over hydrogen atoms, which have an apparent activation energy of 84 and 83.1 kJ/mol for Pt/SO_4^{2-}–ZrO_2 and Pt/MoO_3, respectively. Another similarity between Pt/SO_4^{2-}–ZrO_2 and Pt/MoO_3 is that hydrogen uptake was not appreciable in the absence of Pt. These similarities indicated that the surface sites on both Pt/SO_4^{2-}–ZrO_2 and Pt/MoO_3 have a similar capacity to interact with hydrogen atoms. The difference between Pt/SO_4^{2-}–ZrO_2 and Pt/MoO_3 was observed in the form of the adsorbed hydrogen on the surface of the catalysts. The molecular hydrogen dissociates to form atomic hydrogen, which is followed by the formation of protonic acid sites (H^+) via the release of an electron to a Lewis acid site on the Pt/SO_4^{2-}–ZrO_2. In contrast, it was proposed that the adsorption of hydrogen atoms on the Pt/MoO_3 led to the formation of a hydrogen molybdenum bronze (H_xMoO_3) on the surface of the Pt/MoO_3 catalyst.

The characteristic features of hydrogen adsorption on MoO_3–ZrO_2 are more similar to those of WO_3–ZrO_2 than to those of Pt/SO_4^{2-}–ZrO_2 or Pt/MoO_3. The similarities between MoO_3–ZrO_2 and WO_3–ZrO_2 are described below. The presence of specific sites, such as Pt sites, is not indispensable. At 473 K and above, hydrogen uptake reaches an equilibrium value within 10 h of adsorption. At equilibrium, the hydrogen uptake is lower at higher adsorption temperatures due to the exothermic process of general adsorption. Finally, the rate-controlling step of hydrogen adsorption on the surface of MoO_3–ZrO_2 and WO_3–ZrO_2 was the surface diffusion of the hydrogen atoms, which has an apparent activation energy of 62.8 and 25.9 kJ/mol for MoO_3–ZrO_2 and WO_3–ZrO_2, respectively. This result indicated that the interaction between the hydrogen atoms and the acidic site was stronger for MoO_3–ZrO_2 than for WO_3–ZrO_2. Therefore, the diffusion required more energy on MoO_3–ZrO_2 than on WO_3–ZrO_2.

To elucidate the role of molecular hydrogen-originated protonic acid sites in the *n*-heptane isomerization on the MoO_3–ZrO_2 catalyst, the carrier gas was sequentially switched from hydrogen to nitrogen and back to hydrogen. In the first cycle under a hydrogen stream, MoO_3–ZrO_2 exhibited high activity and stability for *n*-heptane isomerization, and the selectivity for *iso*-heptane and the conversion of *n*-heptane were found to be 44.5 and 31.0%, respectively. In the second cycle, the rate of *n*-heptane conversion decreased by about 85% when the carrier gas was switched from hydrogen to nitrogen. The selectivity for *iso*-heptane was nearly zero for the isomerization in a nitrogen stream with the

Table 1
Product distribution in the isomerization of *n*-heptane over MoO_3–ZrO_2 at 573 K in the presence of hydrogen and nitrogen gases.

	1st cycle (H_2)			2nd cycle (N_2)		3rd cycle (H_2)			
TOS (min)	40	200	360	480	640	800	920	1120	1280
Conversion (%)	30	31	31	31	4.5	5	20	21.7	22
Selectivity (%)									
C_1–C_2	12.9	13.5	13.1	23.2	35	35.5	24	23	22.5
C_3–C_4	15.5	15	14.9	16	45	45.3	17.4	17.2	17
C_5	14.2	14	14.3	15.8	13	13.2	14.6	15.5	16.9
C_6	13.4	13	13.2	10	7	6	17	7.8	6.6
iC_7	44	44.5	44.5	35	0	0	27	36.5	37

increasing of the C_1–C_4 fraction of reaction products. The product distributions in the isomerization of *n*-heptane under hydrogen and nitrogen carrier gases are summarized in Table 1. The decreased catalytic activity resulting from switching the carrier gas to nitrogen may be due to the gradual exhaustion of the protonic acid sites on the surface of the MoO_3–ZrO_2. The absence of molecular hydrogen may prevent the formation of protonic acid sites on the surface of the MoO_3–ZrO_2, resulting in the inhibition of isomerization. The activity and stability of the MoO_3–ZrO_2 recovered slowly with the pulse number when the carrier gas was switched back to hydrogen. Although the activity and stability did not recover completely after switching back to hydrogen, the promotive effect of hydrogen was still observed for the MoO_3–ZrO_2 catalyst. The deactivation of MoO_3–ZrO_2 may be caused by the formation of coke deposits on the surface of the MoO_3–ZrO_2 during the reaction in a nitrogen stream. The promotive effects of hydrogen on the hydrocarbon conversion have been reported by several research groups. Iglesia et al. reported that Pt/WO_3–ZrO_2 showed a high selectivity for *n*-heptane isomerization due to the presence of reduced Pt sites that dissociate dihydrogen and store the H-atoms required for hydrogen transfer and carbocation desorption [29]. Kusakari et al. [30] and Shishido et al. [31] reported the participation of H^+ and H^- from molecular hydrogen produced by the hydrogen spillover mechanism in the hydrocarbon isomerization and cracking over the Pt/SiO_2 + HBeta and Pt/SO_4^{2-}–ZrO_2 catalysts.

5. Summary

1. ESR and IR studies confirmed the formation of protons and electrons from hydrogen molecules on MoO_3–ZrO_2.
2. Hydrogen adsorption on MoO_3–ZrO_2 involves the dissociation of hydrogen molecules to form hydrogen atoms that undergo surface diffusion to form protonic acid sites adjacent to Lewis acid sites.
3. The rate-controlling step for hydrogen adsorption on MoO_3–ZrO_2 is the surface diffusion step, which has an apparent activation energy of 62.8 kJ/mol.
4. The presence of gaseous hydrogen enhanced the activity of MoO_3–ZrO_2 for the isomerization of *n*-heptane.

Acknowledgements

This work was supported by The Ministry of Higher Education, Malaysia through the Fundamental Research Grant Scheme No. 78670 and the UTM Short Term Research Grant No 77330. We also thank the Hitachi Scholarship Foundation for the Gas Chromatograph Instruments Grant.

References

[1] K. Arata, Adv. Catal. 37 (1990) 165–211.
[2] D.G. Barton, S.L. Soled, G.D. Meitzner, G.A. Fuentes, E. Iglesia, J. Catal. 181 (1999) 57–72.
[3] M. Scheithauer, R.K. Grasseli, H. Knoezinger, Langmuir 14 (1998) 3019–3029.
[4] A.S.C. Brown, J.S.J. Hargreaves, S.H. Taylor, Catal. Lett. 57 (1999) 109–113.
[5] J.R. Sohn, E.W. Chun, Y. Pae, Bull. Korean Chem. Soc. 24 (2003) 1785–1792.
[6] M. Khurshid, M.A. Al-Daous, H. Hattori, S.S. Al-Khattaf, Appl. Catal. A 362 (2009) 75–81.
[7] H. Hattori, T. Shishido, Catal. Surv. Jpn. 1 (1997) 205–213.
[8] T. Sugeng, T. Yamada, H. Hattori, Appl. Catal. A: Gen. 242 (2003) 101–109.
[9] N.N. Ruslan, N.A. Fadzlillah, A.H. Karim, A.A. Jalil, S. Triwahyono, Appl. Catal. A: Gen. 406 (2011) 102–112.
[10] N. Satoh, J.-i. Hayashi, H. Hattori, Appl. Catal. A: Gen. 202 (2000) 207–213.
[11] S. Triwahyono, T. Yamada, H. Hattori, Appl. Catal. A: Gen. 250 (2003) 65–73.
[12] P. Afanasiev, Mater. Chem. Phys. 47 (1997) 231–238.
[13] A. Calafat, L. Avilan, J. Alda, Appl. Catal. A: Gen. 201 (2000) 215–223.
[14] K.V.R. Chary, K.R. Reddy, G. Kishan, J.W. Niemantsverdriet, G. Mestl, J. Catal. 226 (2004) 283–291.
[15] J.C. Yori, C.L. Peak, J.M. Parera, Catal. Lett. 64 (2000) 141–146.
[16] K. Arata, Appl. Catal. A: Gen. 146 (1996) 3–32.
[17] C. Kenney, Y. Maham, A.E. Nelson, Thermochim. Acta 434 (2005) 55–61.
[18] S. Triwahyono, Z.A. Abdullah, A. Jalil, J. Nat. Gas. Chem. 15 (2006) 247–252.
[19] S. Triwahyono, T. Yamada, H. Hattori, Catal. Appl. A 250 (2003) 75–81.
[20] S. Triwahyono, A.A. Jalil, H. Hattori, J. Nat. Gas Chem. 16 (2007) 252–257.
[21] S. Triwahyono, A.A. Jalil, S.N. Timmiati, N.N. Ruslan, H. Hattori, Appl. Catal. A 372 (2010) 103–107.
[22] S. Triwahyono, T. Yamada, H. Hattori, Catal. Lett. 85 (2003) 109–115.
[23] M. Occhiuzzi, D. Cordishi, R. Dragone, J. Phys. Chem. 106 (2002) 12464–12469.
[24] Z. Sojka, M. Che, Surf. Chem. Catal. 3 (2000) 163–174.
[25] C. Louis, M. Che, J. Phys. Chem. 91 (1987) 2875–2883.
[26] Q. Zhao, X. Wang, T. Cai, Appl. Surf. Sci. 225 (2004) 7–13.
[27] M. Che, B. Canosa, A.R. Gonzalez-Elipet, J. Chem. Soc. Faraday Trans. 1 (1982) 1043–1050.
[28] H. Al-Kandari, F. Al-Kharafi, N. Al-Awadi, O.M. El-Dusouqui, S.A. Ali, A. Katrib, Appl. Catal. A 295 (2005) 1–10.
[29] E. Iglesia, D.G. Barton, S.L. Soled, S. Miseo, J.E. Baumgartner, W.E. Gates, G.A. Fuentes, G.D. Meitzner, Stud. Surf. Sci. Catal. 101 (1996) 533–542.
[30] T. Kusakari, K. Tomishige, K. Fujimoto, Appl. Catal. A 224 (2002) 219–228.
[31] T. Shishido, H. Hattori, J. Catal. 161 (1996) 194–197.